climate

MDPI

Strategies for Development and Improvement of the Urban Fabric: A Vienna Case Study

Milena Vuckovic [1],* [ID], Aida Maleki [2] and Ardeshir Mahdavi [1]

[1] Department of Building Physics and Building Ecology, TU Wien, Karlsplatz 13, 1040 Vienna, Austria; bpi@tuwien.ac.at
[2] Department of Architecture and Urban Planning, Tabriz Islamic Art University, 51368 Tabriz, East Azarbaijan, Iran; a.maleki@tabriziau.ac.ir
* Correspondence: milena.vuckovic@tuwien.ac.at

Abstract: Numerous studies have shown that densely developed and populated urban areas experience significant anthropogenic heat flux and elevated concentrations of air pollutants and CO_2, with consequences for human health, thermal comfort, and well-being. This may also affect the atmospheric composition and circulation patterns within the urban boundary layer, with consequences for local, regional, and global climate. One of the resulting local implications is the increase in urban air temperature. In this context, the present contribution explores urban fabric development and mitigation strategies for two locations in the city of Vienna, Austria. Toward this end, the potential of specific planning and mitigation strategies regarding urban overheating was assessed using a state-of-the-art CFD-based (computational fluid dynamics) numeric simulation environment. The results display different levels of effectiveness for selected design and mitigation measures under a wide range of boundary conditions.

1. Introduction

1.1. Background

Current projections foresee a vast expansion of global urban population by 2050, with an increase from 60% of the global population living in urban settings in 2030 to 66% by 2050 [1–3]. This development is accompanied by the dynamic growth of cities and its implications in terms of environmental degradation, given the fact that cities and their inhabitants are major contributors to waste heat and CO_2 emissions [4,5]. Numerous studies have shown that densely developed and populated urban areas show significant anthropogenic heat flux [6–10]. This is in part due to the unbalanced integration of urban infrastructure into the urban fabric, namely the transportation network, and multiple systems for heating, cooling, ventilation, and air-conditioning of buildings. Dong et al. (2017) noted that relatively high values of anthropogenic heat flux may be found in large cities of eastern Asia, south and southeastern Asia, Eastern Europe, and the US. A majority of these cities are known to accommodate a dense population that consumes large amounts of energy and requires extensive transportation networks to accommodate cities' emerging needs. The highest value of anthropogenic heat flux (of 493 Wm^{-2}) was recorded within the Hong Kong metropolitan area for the year 2013, for an individual cell of a global model with a spatial resolution of 30 arc-seconds (1 km) and a temporal resolution of 1 h. Further environmental problems associated with higher anthropogenic heat emissions are the elevated concentrations of air pollutants and atmospheric CO_2, which have immediate consequences for human health, thermal comfort, and well-being [11,12]. Such large concentrations of air pollutants and CO_2 substantially influence air quality, and are found

to affect the atmospheric composition and circulation patterns within the urban boundary layer, with potential repercussions for local, regional, and global climate [13–16]. One of the resulting local implications is the increase of outdoor urban air and surface temperature and consequential microclimatic development [8,13,17,18]. Chen et al. (2014) analyzed the distribution and magnitude of the global anthropogenic heat flux and concluded that the anthropogenic heat flux density is large enough to affect local climate change. They further observed the surface temperature increase (of 1–2 K) in the mid and high latitudes of Eurasia and North America, due to the elevated anthropogenic heat release. In turn, elevated outdoor air temperatures have repercussions for energy use for cooling, due to the extensive use of air-conditioning systems, which leads to even more waste heat in the built environment [19]. The extent of these impacts may be exacerbated by dense urban morphologies, higher thermal storage in the built environment, distinct surface cover, and poorly ventilated urban fabric [20,21]. For these reasons, the ongoing rapid urbanization and resulting environmental implications call for an unprecedented commitment to change the way cities evolve.

The spectrum of possibilities for the development and improvement of the urban fabric is rather wide. One approach relates to new urban developments on as yet empty building lots. The other relates to a variety of well-conceived and well-coordinated actions that are aimed at the transformation of existing urban domains. This set of actions is commonly referred to as the mitigation strategies, and they are believed to positively influence the negative phenomena associated with the urban overheating [22]. These efforts usually focus on the reduction of the fraction of energy that is stored within the urban fabric, promotion of the cooling potential of building materials in the physical environment, and enhancement of airflow through the city [23–26]. As these kinds of mitigation measures require substantial resources and major investments, the provision of timely and detailed information regarding the assessment of energy and environmental implications of these measures is, as such, of great importance. In recent years, the research in this field has substantially expanded. An increasing number of these efforts is concerned with the impact assessment analysis of the modification of the building stock, including cool building envelopes, green roofs, and green facades [27–31]. Pisello et al. (2015) [27], for example, observed that the local decrease of external surface temperature of roofs and facades, after the higher albedos materials were applied, was 19.8 K and 9.9 K, respectively, when compared to conventional materials. The combined effect of the two solutions led to the reduction of the indoor operative temperature of 3.1 K. Heusinger and Weber (2015) [28] reported, for a case study in Germany, that the summer surface temperature of a green roof may be 17.4 K lower than of that of a bitumen roof, with a significant reduction of ambient air temperature 0.5 m above roof level. Other efforts are directed toward assessing the environmental implications of specific interventions in the urban landscape, such as the increase in urban vegetation, namely parks and trees, the application of paving materials with higher albedo values, the application of pervious paving materials, and introducing the bodies of water [32–34]. Georgakis et al. (2014) [32] investigated the potential of high reflective coatings used for pavements and walls toward reducing the heat content in urban canyons. They noted a decrease of 8 K of surface temperature, and 1 K of the ambient air temperature inside the urban canyon. Wang and Akbari (2016) [34] discussed the effect of trees on the outdoor thermal environment within the urban canyon in Montreal and documented an air temperature reduction of 4 K at 20 m height from the ground level.

1.2. Overview

Given this background, the present contribution investigates the potential and the implications of specific planning and mitigation strategies regarding urban overheating for two study domains in the city of Vienna, Austria. For this purpose, the following steps were taken:

- First, high-resolution data streams across distinct urban and non-urban locations were obtained, structured, and analyzed. This facilitated the investigation of the microclimatic diversity across these locations. Additionally, this allowed for the identification of essential features of the built

environment that are hypothesized to influence the extent of stored heat in the physical mass of the city.

- Subsequently, we investigated the potential of specific mitigation strategies to remedy the negative phenomena associated with urban overheating. For this purpose, three mitigation strategies were considered for the targeted high-density urban area: (i) planting trees, (ii) greening of the roofs, (iii) combination of both measures. These measures were selected based on their potential as a viable mitigation strategy that can be conveniently integrated into the existing urban fabric, their potential for generating both short- and long-term mitigation effects in urban areas, and their compatibility with local climatic conditions. To facilitate the environmental impact assessment of these measures, comprehensive simulations were carried out using the state-of-the-art CFD-based numeric simulation environment ENVI-met [35].

- Additionally, we investigated the microclimatic consequences of a proposed urban development in an existing abandoned industrial site using the same numeric simulation environment.

## 2. Methodology

2.1. Microclimate Development in Vienna

As stated at the outset, higher anthropogenic heat emissions, resulting from rapidly increasing urban population and emerging energy needs, may influence the atmospheric composition and circulation patterns within the urban boundary layer. In turn, this may have potential consequences for local climate, specifically for elevated ambient air temperature. To illustrate this development, we conducted a comprehensive microclimatic investigation of a number of distinct low-density and high-density urban and non-urban (outside the metropolitan area) segments within the city of Vienna (see Figure 1 and Table 1). In our previous research efforts, we developed advanced Python-based spatial algorithms implemented in a GIS environment to derive a set of morphological and physical parameters for these locations, for a spatial dimension of 400 m, as described in [36–41] and seen in Table 1.

In order to investigate the microclimatic behavior of selected urban and non-urban locations, we obtained hourly-based meteorological information pertaining to air temperature, wind speed, solar radiation, and precipitation from five weather stations centrally positioned within these areas. These stations are operated by the Central Institution for Meteorology and Geodynamics (Zentralanstalt für Meteorologie und Geodynamik, ZAMG) [42]. These stations provide continuous data at frequent intervals, where reliability of meteorological observations is assured via a thorough quality control using the QualiMET system and according to the WMO guidelines [43]. Additionally, the correction of the hourly-based data is performed using GEKIS (Geografisches Klimainformationssystem—Geographic Climate Information System). With approximately 250 semi-automatic weather stations (Teil Automatisches Wetter Erfassungs System—TAWES) spatially distributed throughout Austria, the coverage of the ZAMG network is rather extensive, with denser networks in populated areas [42].

The acquired meteorological information was further processed into four hourly-based reference days, representing typical weather conditions of each season for the year 2012. Thereby, the hourly data on air temperature and wind speed was averaged over a continuous three-week period identified for each meteorological season. These representative periods were characterized by a stable air mass free of excessive changes in pressure and airflow velocity (less than 3 m·s^{-1}), with little or no precipitation, thus allowing us to investigate micro-level changes in urban climate. It should be noted that the data selection process was performed for the area of the highest urban density (IS). Subsequently, the same time frame was applied for other areas. In order to compare wind speed readings taken from different heights, as seen in Table 1, we used the Hellmann exponential law to estimate the wind speed at street level (1.1 m above ground) [44]:

$$\frac{v}{v_{\text{n}}} = \left(\frac{H}{H_{\text{n}}}\right)\alpha \tag{1}$$

where v is the wind speed at height H = 1.1 m, v_n is the wind speed at height H_n (height of the observations), and α is the friction coefficient (Hellmann exponent). The friction coefficient used for this study is as follows: 0.25 for non-urban and low-density suburban areas (SEI and MB, respectively), 0.30 for mid-density suburban areas (HW and DF), and 0.40 for the high-density urban area (IS).
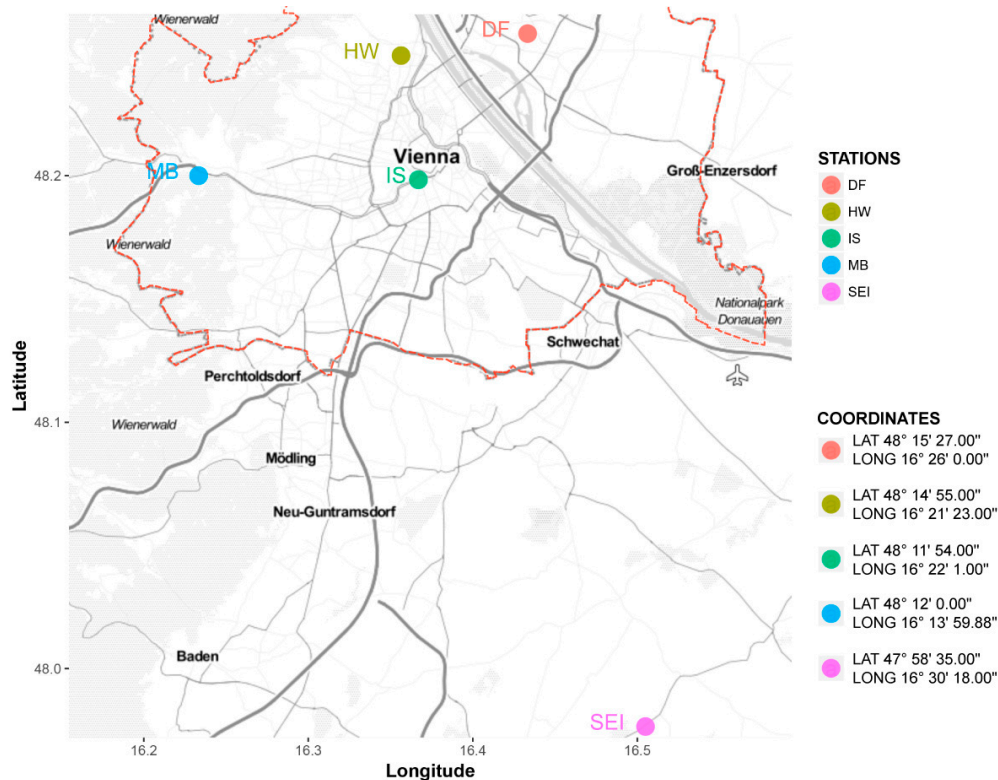
Figure 1. Selected locations and the respective weather stations within (DF, HW, IS, MB). And outside (SEI) Vienna (red dashed line marks the boundary of the metropolitan area).

Table 1. Information on selected weather stations.

Name	LCZ [1]	Temperature Sensor Height (m)	Wind Sensor Height (m)	Built Area Fraction [2]	Average Building Height [m]	Q_f [kWh/m²a¹]
IS	LCZ 2	9.3	52	0.41	23.35	350
HW	LCZ 6	1.9	35	0.18	8.00	177
DF	LCZ 6	2	13	0.20	6.15	89
MB	LCZ 9	2.1	9.5	0.04	5.23	70
SD	LCZ 8$_D$	2.1	15	0.08	5.29	67

[1] LCZ stands for Local Climate Zone, a classification system devised by Stewart and Oke (2012) [45]. [2] Q_f denotes the mean annual heat flux density from fuel combustion and human activity. More detailed information regarding the concerned parameters can be found in [37].

2.2. Strategies for Development and Improvement of the Urban Fabric

Current transformations of the physical environment, such as the increased building density, abundance of sealed surfaces, and reduced vegetation fraction lead to, among other things, significant heat storage in the urban fabric (i.e., building surfaces, pavements, and roads). As such, the study of strategies for improvement of the urban fabric holds great potential, with important sustainability implications. However, these strategies may prove effective only if a comprehensive body of scientific knowledge and expertise supports their realization.

As a contribution to the ongoing research efforts in this direction, we focus on a comprehensive environmental impact assessment of a number of mitigation and urban development strategies using

a numerical model, ENVI-met version 4.0 [35]. ENVI-met is a 3-dimensional non-hydrostatic model specifically tailored for the simulation of surface-plant-air interactions within urban environments. The capabilities of this tool to facilitate the assessment of complex and non-linear interactions between the surrounding urban fabric and local climatic context have been broadly documented by the scientific community [46–48]. However, as with other areas of applied numerical modelling, certain issues related to the reliability of the model must be addressed. Thereby, in our previous research efforts we have documented the model calibration potential toward improved performance, as described in [49].

Three mitigation strategies were considered for the targeted area IS: (i) planting trees, (ii) greening of the roofs, (iii) combination of both measures (Figure 2). This area was selected as it is the most developed part of the city with high traffic intensity, hence it has a tendency toward higher urban overheating. For the trees, we considered deciduous trees of an average height of 13 m, C3-type, with an average albedo value of 0.2, average crown width of 9 m, and a LAD (Leaf Area Density) ranging from 0.5 to 2. More specifically, C3-type plants are referred to as the temperate or cool-season plants that are most efficient at photosynthesis in cool, wet climates [50]. Some examples include evergreen trees, deciduous trees and weed-like plants. For the green roofs we considered semi-intensive systems of an average vegetation height of 0.18 m, C3-type, and with an albedo value of 0.2. Four sets of simulation runs were conducted for a base case and for each scenario using the previously derived hourly-based seasonal reference days as boundary conditions. The input model assumptions are presented in Table 2. The possibility of user-defined diurnal variations of atmospheric boundary conditions (hourly forcing) offered in ENVI-met version 4.0 was used.

Once the high-resolution modelling output was generated, the sensitivity of ambient outdoor air temperature (sampled from the height of 1.8 m above the ground) to various mitigation strategies was investigated. For this purpose, the concept of Cumulative Temperature Decrease (CTD) [38] was used as the thermal performance indicator. CTD (Kh) denotes the sum of the hourly differences between the air temperature of a base case ($\theta_{B,i}$) and respective mitigation scenarios ($\theta_{M,i}$) over a specific period of time (e.g., over a day), whereby only positive differences ($\theta_{B,i} > \theta_{M,i}$) were considered:

$$\mathrm{CTD} = \sum_{i=1}^{24} (\theta_{B,i} - \theta_{M,i}) \quad \text{for } \theta_{B,i} >_{M,i} \tag{2}$$

In order to investigate the temporal scale of the potential thermal benefits of each mitigation strategy, CTD values were further represented for nighttime (the period between the sunset and sunrise) and daytime (the period between sunrise and the sunset). The variation in daylight hours was adopted from the annual sun path diagram for the city of Vienna and rounded to the whole hour, as seen in Table 3 [51].

Additionally, we investigated the implications of a new large-scale design and renovation proposal for a local microclimate. The study area, called Nordbahnhof, represents an abandoned industrial site, currently a brownfield, located on the periphery of the urban center of the city of Vienna. The area is targeted for new urban redevelopment, specifically the construction of a new residential complex with a building height in the range of 10 to 70 m (Figure 3). The meteorological information for this area was provided by the Municipal Department of Environmental Protection in Vienna, MA22 [52]. The MA22 network comprises 17 monitoring weather stations distributed throughout the metropolitan area of the city of Vienna. These stations are calibrated following the ÖNORM standards (national standards published by the Austrian Standards Institute). Monitoring data storage and quality check procedures are based on ON/EN/ISO standards, which are recognized by WMO. The same input model assumptions as presented in Table 2, were applied for this case, except of the initial temperature at the upper soil layer, which was recalculated.
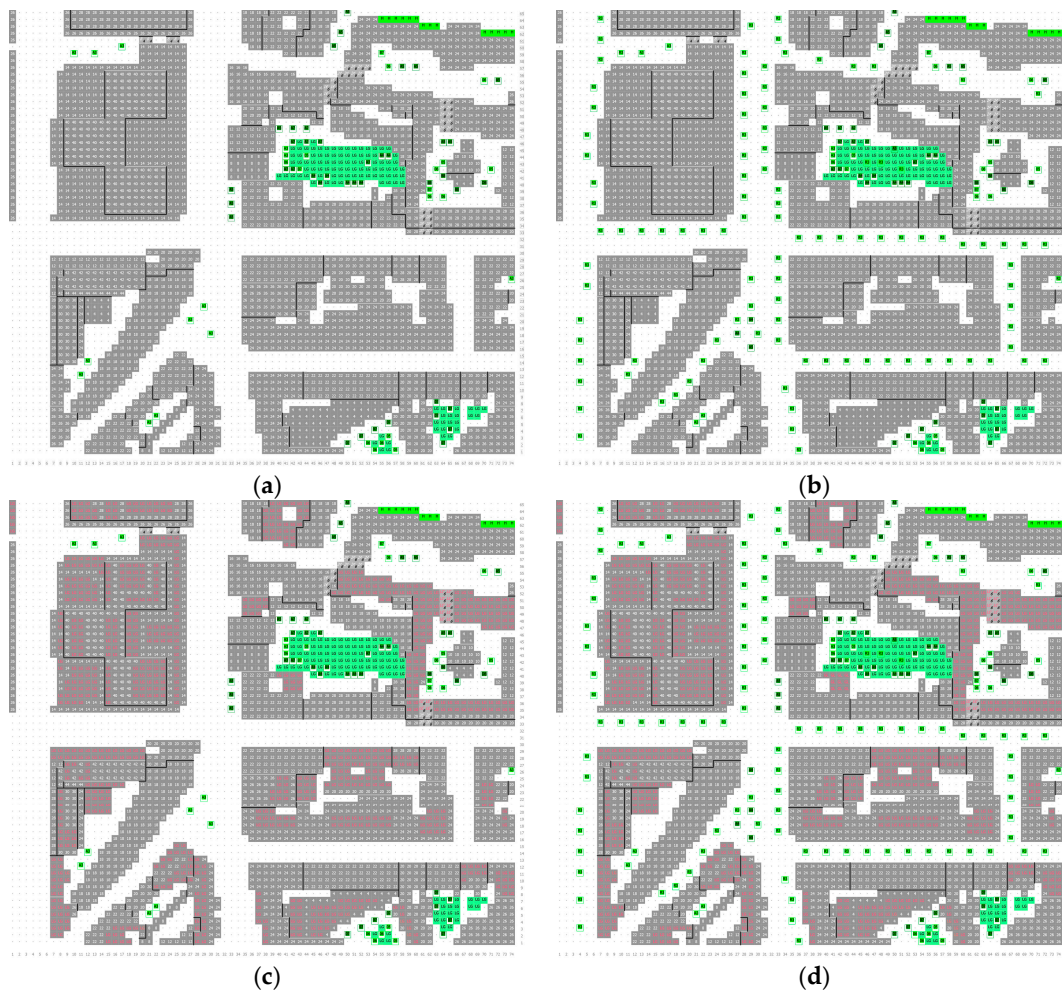
Figure 2. Schematic illustration of the envisioned mitigation strategies implemented in ENVI-met: (**a**) base case, (**b**) trees, (**c**) green roofs (in red), (**d**) combined.

Table 2. Input model assumptions for location IS.

Parameter	Unit	Winter	Spring	Summer	Autumn
Total simulation time	h	48	48	48	48
Grid size	m	4	4	4	4
Adjustment factor for solar radiation	-	0.82	0.82	0.82	0.82
Specific humidity at 2500 m	g Water/kg air	3	7	8	6
Initial temperature at the upper soil layer (0–20 cm)	K	275	290	293	281
Turbulence scheme for 1D reference model/3D main model	-	Prognostic (TKE closure)			
Roughness length z_0 at reference point	m	0.1	0.1	0.1	0.1

For the parameters not listed in Table 2, default system settings were used.

Table 3. Daylight hours for each season.

Time	Winter	Spring	Summer	Autumn
Reference day	22 February	4 May	5 August	5 November
Daylight	07:00–17:00	05:00–20:00	06:00–20:00	07:00–16:00

(**a**) (**b**)

**Figure 3.** Nordbahnhof area: (**a**) base case, (**b**) new urban development.

3. Results and Discussion

Figure 4 illustrates the ambient air temperature and wind speed for the winter and summer reference days for the selected locations. These results demonstrate significant variation in the distribution of observed meteorological parameters across time (season) and space (location). Generally, the central urban area (IS) had the smallest diurnal temperature range, with the highest daily maximum, median, and minimum values, for both winter and summer periods. The highest minimum value demonstrates the reduced nighttime cooling potential of densely developed urban areas. Moreover, looking at the inter-quartile range (IQR) for location IS for the summer period, the median is shifted toward the lower quartile with a wider spread of individual observations in the upper quartile compared to the clustering of observations in the lower quartile. This implies a somewhat larger tendency toward extreme values for higher temperatures.

The wind speed data shows a substantial decrease in airflow in location IS for both seasons. Although this may be considered positive in cold seasons (e.g., lower building heating demands, higher outdoor thermal comfort), it may have a negative impact in summer due to urban overheating. These results underline the significant potential of mitigation measures specifically in the IS location.

Figure 5 illustrates, for area IS, the mean hourly air temperature difference between the base case and three mitigation scenarios in the course of seasonal reference days. Figure 6 illustrates the computed daytime and nighttime CTD values of the envisioned mitigation strategies over four seasons. The results point to the different levels of impact of selected mitigation measures under a wide range of boundary weather conditions. In general, the consideration of trees prove to be quite beneficial for the improvement of thermal conditions in the urban canyon, especially during the summer period. The degree of improvement over day- and nighttime periods appears to be, however, dependent on the season. Higher daytime air temperature reductions (Δq) and CTD values were observed during warmer months, while the opposite was true for colder months. This occurrence may be explained,

on one hand, by the overall higher solar gain and resulting increased effect of radiation shielding by trees during the summer period, thus pointing to the valuable role of tree shade. On the other hand, deciduous trees provide significantly less shade in the colder months due to the loss of leaves, allowing solar access to horizontal and vertical surfaces (mainly pavements, roads, and building walls), thus maximizing the absorption of heat from solar radiation. This in turn may have important positive consequences for building heating demands. Higher Δq and CTD values were also observed during the nighttime, for both colder and warmer months. As the overall solar gain was reduced during the day due to the shading effect of the trees, there was substantially less heat absorbed in the urban fabric, thus making the temperature difference from the base case larger.
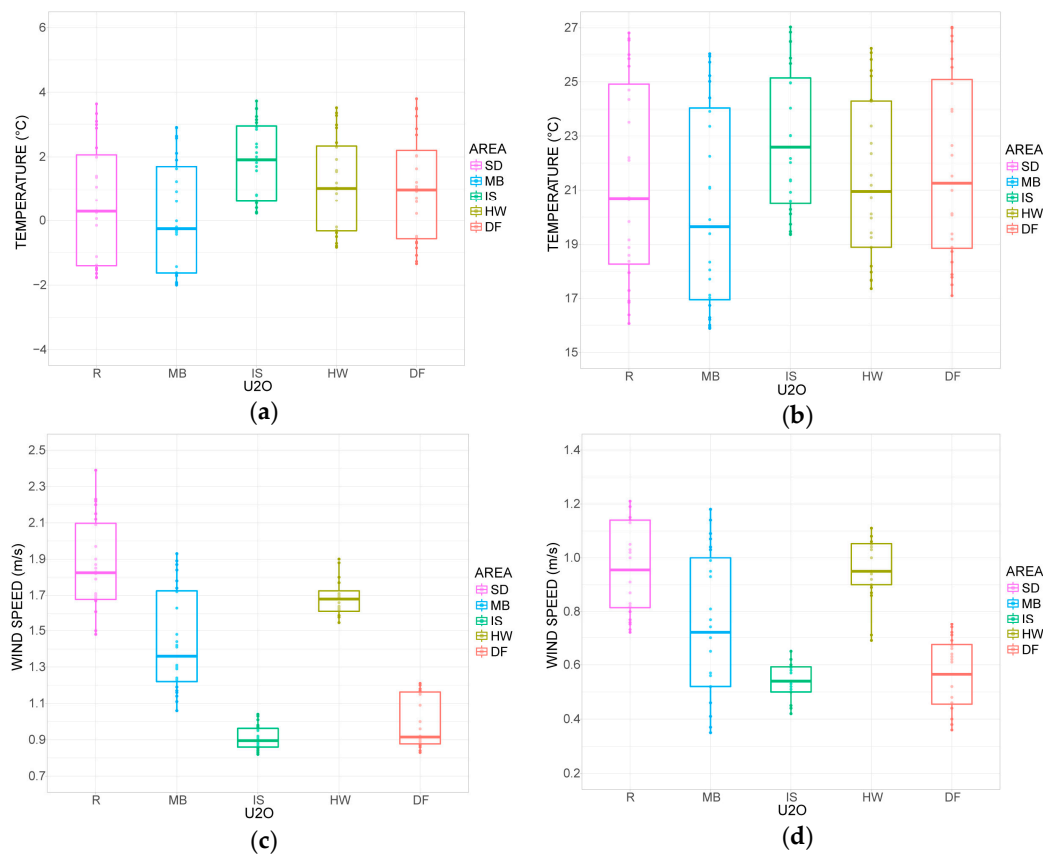

Figure 4. Boxplots of ambient air temperature and wind speed data for a reference day in summer and winter periods, with individual hourly data points: (**a**) winter temperature, (**b**) summer temperature, (**c**) winter wind speed, (**d**) summer wind speed.

The implementation of green roofs appears to have little or no effect on the thermal conditions within the urban canyon. This may be attributed to the relatively high elevation of vegetative elements, thus limiting the effect on data sampled from the street level. Green roofs are generally more important for their effect on the boundary layer conditions due to the overall lower storage heat flux than in conventional roof constructions. This, in turn, leads to less energy available for release back into the atmosphere and results in cooler air masses above the roof surface. This circumstance is specifically relevant for reductions of near-surface and surface roof temperatures. Additionally, green roofs provide better roof insulation, with a significant impact on a building's energy use.

As it could be expected, the results suggest that, in the case of the study area in Vienna, a combination of the two measures had the largest positive effect on urban overheating. It can thus be concluded that the concurrent deployment of multiple intervention measures whose mitigation mechanisms vary in temporal scale and magnitude may amplify the discrete effects of a single measure.
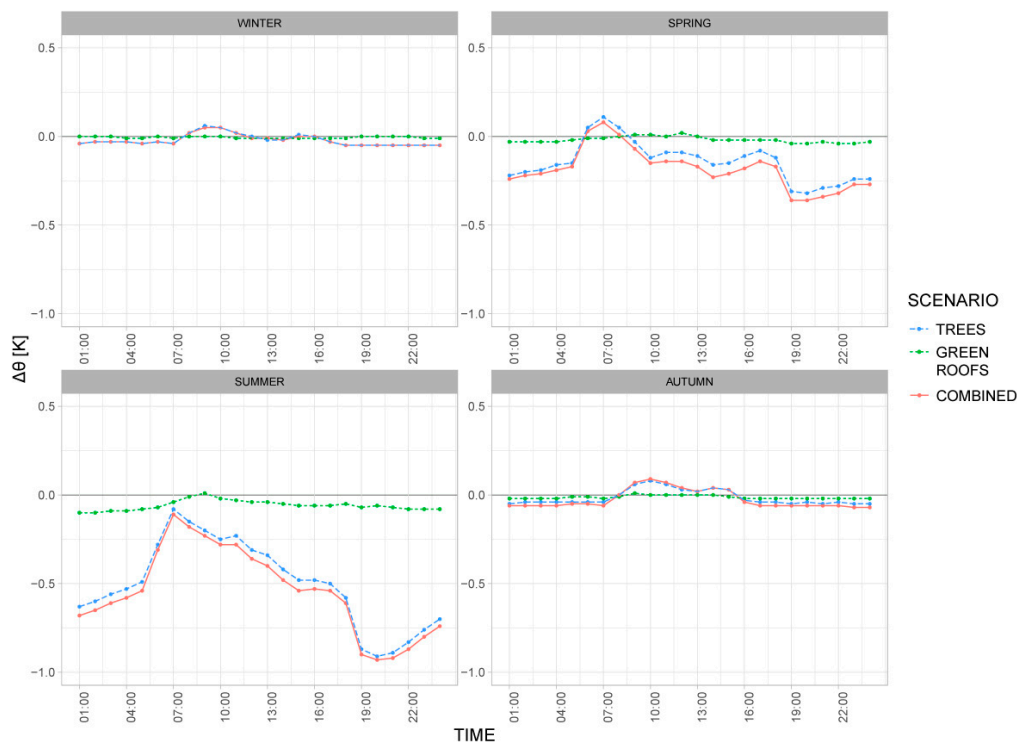
Figure 5. Mean hourly air temperature difference between the base case and three mitigation scenarios in the course of seasonal reference days, area IS.
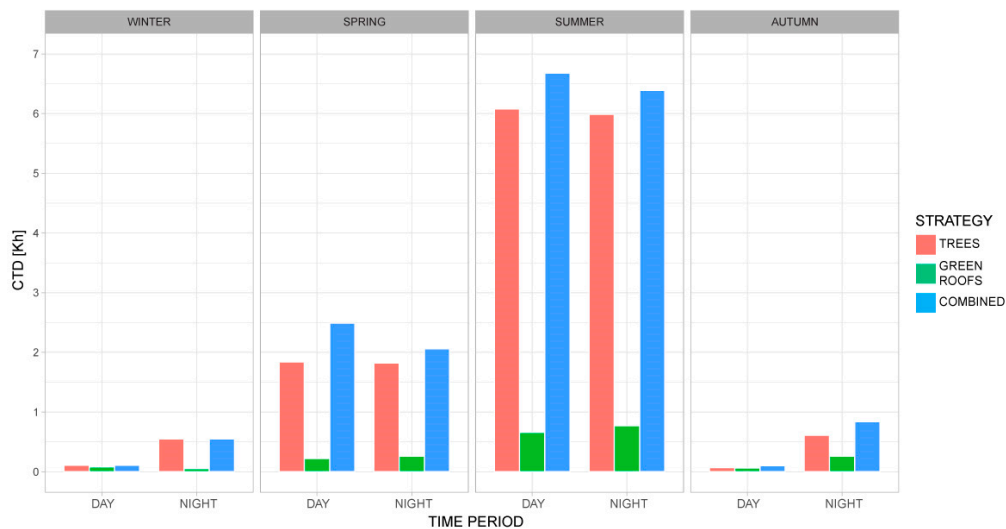

Figure 6. Computed daytime and nighttime Cumulative Temperature Decrease (CTD) values for envisioned mitigation strategies for the targeted area IS.

Lastly, we investigated the resulting climatic effect of distinct transformations of the urban landscape. The computed daytime and nighttime seasonal CTD values for the Nordbahnhof area are presented in Table 4. Figure 7 illustrates the mean seasonal hourly air temperature of the base case (brownfield) and the development scenario for the Nordbahnhof area. The results point to a varying effect on the thermal environment across both the day-night cycle and the season. Namely, a diurnal cooling effect may be observed during warmer months (up to 1.6 K). This is in part due to the shadowing effect caused by new tall buildings, limiting the incidence of direct solar radiation on the neighboring buildings and the ground surface. Consequently, less heat was stored in the physical

mass of built structures and eventually re-emitted back into the environment, leading to cooler local surroundings. However, as this might be seen as an opportunity to increase the shade in summer, during the winter it might affect the insolation potential of the area.

Table 4. Computed daytime and nighttime CTD values for Nordbahnhof area.

CTD [Kh]	Winter	Spring	Summer	Autumn
Day	0	6.5	12.7	0
Night	0	0	0.33	0
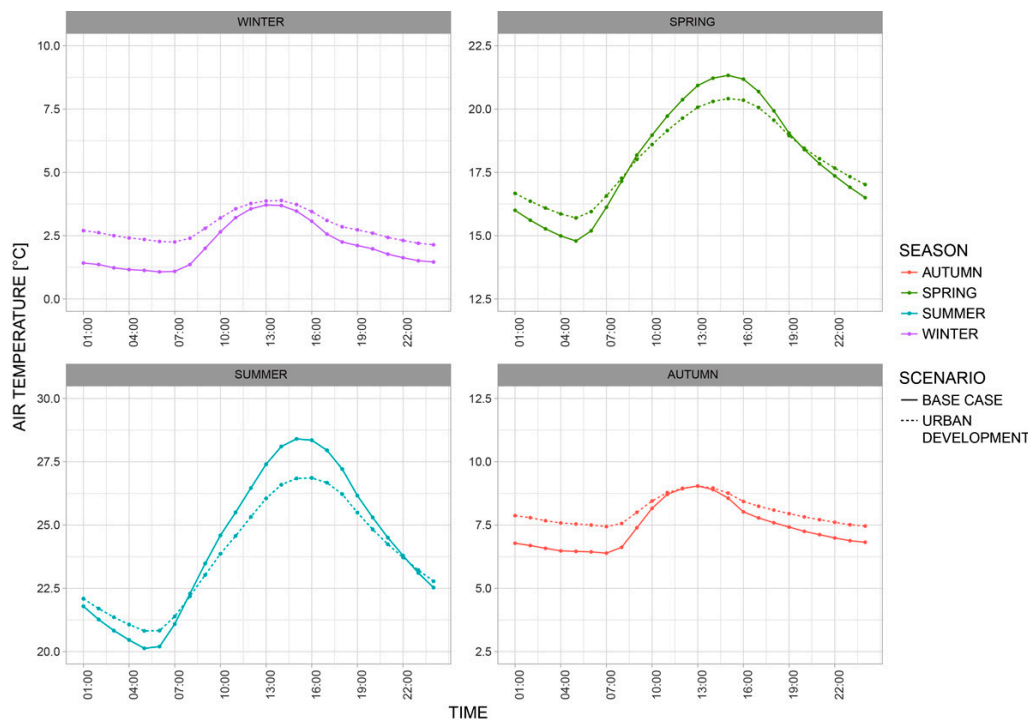
Figure 7. Mean hourly air temperature of the base case and development scenario for each season, Nordbahnhof area.

Additionally, a nocturnal heating effect was observed for each season, ranging from 0.7 to 1.3 K. This is to be expected due to the higher fraction of built surfaces with high thermal admittance and, therefore, the higher thermal mass of the area compared to the base case. This resulted in a greater fraction of heat being stored within the urban fabric. In turn, the heat loss from within the urban canyons was hampered due to the lower sky view factor (SVF). The effect appears to be more pronounced during the colder months. This might be due to the obstructed cold winter winds by buildings and vegetation, causing a greater departure from the base case conditions.

4. Conclusions

The identification of appropriate urban intervention strategies to mitigate the negative effects of urban overheating is a necessary step towards more sustainable urban environments. In this light, the first objective of our research effort was to contribute to the understanding of the very drivers behind the warming of the cities. It was concluded that areas of higher urban density and higher built surface fraction tend to store more heat during the day. Due to their dense arrangement of built structures, these areas also display a substantial decrease of airflow and are thus prone to more extreme and unfavorable thermal conditions.

One important aspect of our further inquiry was to investigate the potential of a number of mitigation strategies to remedy the negative effects of this process. Thereby, urban trees have been identified as a promising strategy for the improvement of thermal conditions in the urban canyon, leading to a maximum of 6 K summertime air temperature decrease due to their shading properties. Green roofs, on the other hand, had little (around 0.3 K decrease) or no effect on thermal conditions within the urban canyon. The combination of both intervention alternatives proved, in case of Vienna, to be the most effective strategy. Therefore, our results suggest that the application of multiple mitigation strategies may prove more effective if deployed concurrently, rather than in isolation.

Planting urban trees can be argued to be a relatively low-cost, easy-to-implement, and climatically efficient measure against urban overheating. The application of a vegetation layer to building envelopes, more specifically to roof surfaces, may be more financially intensive and, in practice, more difficult to implement due to the issues of private property ownership. Thus, the implementation of urban trees might be the strategy that local authorities would more readily adopt.

Lastly, we investigated the climatic response of a new urban development in an existing abandoned industrial site. The simulation results suggested a post-development diurnal cooling effect of up to 1.6 K (for the spring and summer periods) and an all-year nocturnal heating effect of up to 1.3 K. This is due to the obstructed solar access and airflow by new tall buildings and vegetation. Daytime temperature reduction can be attributed to the solar shielding effect, whereas reduced nighttime cooling potential results in higher temperatures.

There are many potential applications of the presented research and related insights. In general, the outcome of our research effort is expected to advance the local urban development concepts and techniques towards more effective planning practices. Specifically, it was shown that the consideration of climatic knowledge, and understanding the essential urban energy balance concepts can support decision making at the urban level.

Author Contributions: Milena Vuckovic prepared the input weather data for simulations, conducted data analysis and interpreted the results, and contributed substantially to the writing of the manuscript. Aida Maleki performed the simulations. Ardeshir Mahdavi provided general supervision and significant provision of ideas during the project run, and revised the manuscript critically prior the final submission.

Conflicts of Interest: The authors declare no conflict of interest.

References

1. World Health Organization (WHO). *Global Report on Urban Health: Equitable, Healthier Cities for Sustainable Development*; World Health Organization: Geneva, Switzerland, 2016; Available online: http://www.who.int/iris/handle/10665/204715 (accessed on 10 December 2017).
2. United Nations, Department of Economic and Social Affairs, Population Division. *World Urbanization Prospects: The 2014 Revision, Highlights (ST/ESA/SER.A/352)*; United Nations: New York, NY, USA, 2014.
3. United Nations, Department of Economic and Social Affairs, Population Division. *World Population Prospects: The 2015 Revision, Key Findings and Advance Tables*; Working Paper No. ESA/P/WP.241; United Nations: New York, NY, USA, 2015.
4. Wilson, B.; Chakraborty, A. The Environmental Impacts of Sprawl. *Sustainability* **2013**, *5*, 3302–3327. [CrossRef]
5. The European Parliament and the Council of the European Union (EUROPA). Directive 2010/31/EU on the Energy Performance of Buildings. Official Journal of the European Union L 153/13-33. Available online: http://www.buildup.eu/en/practices/publications/directive-201031eu-energy-performance-buildings-recast-19-may-2010 (accessed on 10 December 2017).
6. Harlan, S.L.; Ruddell, D.M. Climate change and health in cities: Impacts of heat and air pollution and potential co-benefits from mitigation and adaptation. *Curr. Opin. Environ. Sustain.* **2011**, *3*, 126–134. [CrossRef]
7. Dong, Y.; Varquez, A.C.G.; Kanda, M. Global anthropogenic heat flux database with high spatial resolution. *Atmos. Environ.* **2017**, *150*, 276–294. [CrossRef]

8. Murray, J.; Heggie, D. From urban to national heat island: The effect of anthropogenic heat output on climate change in high population industrial countries. *Earth's Future* **2016**, *4*, 298–304. [CrossRef]

9. Feng, J.-M.; Wang, Y.-L.; Ma, Z.-G.; Liu, Y.-H. Simulating the Regional Impacts of Urbanization and Anthropogenic Heat Release on Climate across China. *J. Clim.* **2012**, *25*, 7187–7203. [CrossRef]

10. Sailor, D.J.; Georgescu, M.; Milne, J.M.; Hart, M.A. Development of a national anthropogenic heating database with an extrapolation for international cities. *Atmos. Environ.* **2015**, *118*, 7–18. [CrossRef]

11. Ryu, Y.-H.; Baik, J.-J.; Lee, S.-H. Effects of anthropogenic heat on ozone air quality in a megacity. *Atmos. Environ.* **2013**, *80*, 20–30. [CrossRef]

12. Asikainen, A.; Pärjälä, E.; Jantunen, M.; Tuomisto, J.T.; Sabel, C.E. Effects of Local Greenhouse Gas Abatement Strategies on Air Pollutant Emissions and on Health in Kuopio, Finland. *Climate* **2017**, *5*, 43. [CrossRef]

13. Zhang, G.J.; Cai, M.; Hu, A. Energy consumption and the unexplained winter warming over northern Asia and North America. *Nat. Clim. Chang.* **2013**, *3*, 466–470. [CrossRef]

14. Stott, P.A.; Stone, D.A.; Allen, M.R. Human contribution to the European heatwave of 2003. *Nature* **2004**, *432*, 610–614. [CrossRef] [PubMed]

15. Krpo, A.; Salamanca, F.; Martilli, A.; Clappier, A. On the Impact of Anthropogenic Heat Fluxes on the Urban Boundary Layer: A Two-Dimensional Numerical Study. *Bound.-Layer Meteorol.* **2010**, *136*, 105–127. [CrossRef]

16. Chen, Y.; Jiang, W.M.; Zhang, N.; He, X F.; Zhou, R.W. Numerical simulation of the anthropogenic heat effect on urban boundary layer structure. *Theor. Appl. Climatol.* **2008**, *97*, 123–134. [CrossRef]

17. Erell, E.; Pearlmutter, D.; Williamson, T.J. *Urban Microclimate: Designing the Spaces between Buildings*, 1st ed.; Earthscan: London, UK, 2011.

18. Chen, B.; Dong, L.; Shi, C.; Li, L.-J.; Chen, L.-F. Anthropogenic Heat Release: Estimation of Global Distribution and Possible Climate Effect. *J. Meteorol. Soc. Jpn.* **2014**, *92*, 157–165. [CrossRef]

19. Crutzen, P. New directions: the growing urban heat and pollution "island" effect- impact on chemistry and climate. *Atmos. Environ.* **2004**, *38*, 3539–3540. [CrossRef]

20. Grimmond, C.S.B. Urbanization and global environmental change: local effects of urban warming. *Cities Glob. Environ. Chang.* **2007**, *173*, 83–88. [CrossRef]

21. Zhao, C.; Fu, G.; Liu, X.; Fu, F. Urban planning indicators, morphology and climate indicators: A case study for a north-south transect of Beijing, China. *Build. Environ.* **2011**, *46*, 1174–1183. [CrossRef]

22. Gago, E.J.; Roldan, J.; Pacheco-Torres, R.; Ordóñez, J. The city and urban heat islands: A review of strategies to mitigate adverse effects. *Renew. Sustain. Energy Rev.* **2013**, *25*, 749–758. [CrossRef]

23. Aleksandrowicz, O.; Vuckovic, M.; Kiesel, K.; Mahdavi, A. Current trends in urban heat island mitigation research: Observations based on a comprehensive research repository. *Urban Clim.* **2017**, *21*, 1–26. [CrossRef]

24. Santamouris, M. Heat Island Research in Europe: The State of the Art. *Adv. Build. Energy Res.* **2007**, *1*, 123–150. [CrossRef]

25. Santamouris, M. Cooling the cities—A review of reflective and green roof mitigation technologies to fight heat island and improve comfort in urban environments. *Solar Energy* **2014**, *103*, 682–703. [CrossRef]

26. Hebbert, M.; Webb, B. Towards a Liveable Urban Climate: Lessons from Stuttgart. In *Liveable Cities: Urbanising World*; Routledge: New York, NY, USA, 2012; pp. 132–150.

27. Pisello, A.L.; Castaldo, V.L.; Piselli, C.; Pignatta, G.; Cotana, F. Combined Thermal Effect of Cool Roof and Cool Façade on a Prototype Building. *Energy Procedia* **2015**, *78*, 1556–1561. [CrossRef]

28. Heusinger, J.; Weber, S. Comparative microclimate and dewfall measurements at an urban green roof versus bitumen roof. *Build. Environ.* **2015**, *92*, 713–723. [CrossRef]

29. Cameron, R.W.F.; Taylor, J.E.; Emmett, M.R. What's 'cool' in the world of green façades? How plant choice influences the cooling properties of green walls. *Build. Environ.* **2014**, *73*, 198–207. [CrossRef]

30. Berardi, U.; GhaffarianHoseini, A.H.; GhaffarianHoseini, A. State-of-the-art analysis of the environmental benefits of green roofs. *Appl. Energy* **2014**, *115*, 411–428. [CrossRef]

31. Akbari, H.; Kolokotsa, D. Three decades of urban heat islands and mitigation technologies research. *Energy Build.* **2016**, *133*, 834–842. [CrossRef]

32. Georgakis, Ch.; Zoras, S.; Santamouris, M. Studying the effect of "cool" coatings in street urban canyons and its potential as a heat island mitigation technique. *Sustain. Cities Soc.* **2014**, *13*, 20–31. [CrossRef]

33. Gunawardena, K.R.; Wells, M.J.; Kershaw, T. Utilising green and bluespace to mitigate urban heat island intensity. *Sci. Total Environ.* **2017**, *584*, 1040–1055. [CrossRef] [PubMed]

34. Wang, Y.; Akbari, H. The effects of street tree planting on Urban Heat Island mitigation in Montreal. *Sustain. Cities Soc.* **2016**, *27*, 122–128. [CrossRef]

35. Huttner, S.; Bruse, M. Numerical modelling of the urban climate—A preview on ENVI-met 4.0. In Proceedings of the 7th International Conference on Urban Climate ICUC-7, Yokohama, Japan, 29 June–3 July 2009.

36. Vuckovic, M.; Kiesel, K.; Mahdavi, A. The extent and implications of the microclimatic conditions in the urban environment: A Vienna case study. *Sustainability* **2017**, *9*, 177. [CrossRef]

37. Vuckovic, M.; Kiesel, K.; Mahdavi, A. Toward advanced representations of the urban microclimate inbuilding performance simulation. *Sustain. Cities Soc.* **2016**, *27*, 356–366. [CrossRef]

38. Mahdavi, A.; Kiesel, K.; Vuckovic, M. Methodologies for UHI analysis. In *Counteracting Urban Heat Island Effects in a Global Climate Change Scenario*; Musco, F., Ed.; Springer: Berlin, Germany, 2016; pp. 71–91. [CrossRef]

39. QGIS 2.10. Available online: www.qgis.org/ (accessed on 1 September 2017).

40. Glawischnig, S.; Kiesel, K.; Mahdavi, A. Feasibility analysis of open-government data for the automated calculation of the micro-climatic attributes of Urban Units of Observation in the city of Vienna. In Proceedings of the 2nd ICAUD International Conference in Architecture and Urban Design, Epoka University, Tirana, Albania, 8–10 May 2014.

41. Glawischnig, S.; Hammerberg, K.; Vuckovic, M.; Kiesel, K.; Mahdavi, A. A case study of geometry-based automated calculation of microclimatic attributes. In Proceedings of the 10th European Conference on Product and Process Modelling, Vienna, Austria, 17–19 September 2014.

42. ZAMG, Zentralanstalt für Meteorologie und Geodynamik. Available online: http://www.zamg.ac.at (accessed on 1 September 2017).

43. Svensson, P.; Björnsson, H.; Samuli, A.; Andresen, L.; Bergholt, L.; Tveito, O.E.; Agersten, S.; Pettersson, O.; Vejen, F. *Quality Control of Meteorological Observations, Description of potential HQC Systems*; met.no Report; Norwegian Meteorological Institute: Oslo, Norwegian, 2004.

44. Bañuelos-Ruedas, F.; Angeles-Camacho, C.; Rios-Marcuello, S. Methodologies Used in the Extrapolation of Wind Speed Data at Different Heights and Its Impact in the Wind Energy Resource Assessment in a Region. In *Wind Farm—Technical Regulations, Potential Estimation and Siting Assessment*; Suvire, G.O., Ed.; InTech: Rijeka, Croatia, 2011; p. 246.

45. Stewart, I.D.; Oke, T.R. Local Climate Zones for Urban Temperature Studies. *Bull. Am. Meteorol. Soc.* **2012**, *93*, 1879–1900. [CrossRef]

46. Salata, F.; Golasi, I.; De Lieto Vollaro, R.; De Lieto Vollaro, A. Urban microclimate and outdoor thermal comfort. A proper procedure to fit ENVI-met simulation outputs to experimental data. *Sustain. Cities Soc.* **2016**, *26*, 318–343. [CrossRef]

47. Huttner, S.; Bruse, M.; Dostal, P. Using ENVI-met to simulate the impact of global warming on the microclimate in central European cities. In *Berichte des Meteorologischen Instituts der Albert-Ludwigs-Universität Freiburg Nr. 18 (2008), Proceedings of the 5th Japanese-German Meeting on Urban Climatology, Albert-Ludwigs-University of Freiburg, Freiburg, Germany, 6–8 October 2008*; Mayer, H., Matzarakis, A., Eds.; Self-Publishing Company of the Meteorological Institute, Albert-Ludwigs-University of Freiburg: Freiburg, Germany, 2008; pp. 307–312.

48. Gusson, C.S.; Duarte, D.H.S. Effects of Built Density and Urban Morphology on Urban Microclimate—Calibration of the Model ENVI-met V4 for the Subtropical Sao Paulo, Brazil. *Procedia Eng.* **2016**, *169*, 2–10. [CrossRef]

49. Maleki, A.; Kiesel, K.; Vuckovic, M.; Mahdavi, A. Empirical and computational issues of microclimate simulation. *Inf. Commun. Technol. Lect. Notes Comput. Sci.* **2014**, *8407*, 78–85. [CrossRef]

50. Still, C.J.; Berry, J.A.; Collatz, G.J.; DeFries, R.S. Global distribution of C3 and C4 vegetation: Carbon cycle Implications. *Glob. Biogeochem. Cycles* **2003**, *17*, 1006. [CrossRef]

51. Yearly Sun Graph. Available online: www.timeanddate.com/sun/austria/vienna (accessed on 1 December 2017).

52. MA22, 2015. Magistrat der Stadt Wien—Die Wiener Umweltschutzabteilung (Municipal Department 22—Environmental Protection in Vienna). Available online: www.umweltschutz.wien.at (accessed on 1 Spetember 2017).